Liquid Chromatography

DOI: 10.1002/anie.201201096

A Molecular Dynamics Study on the Partitioning Mechanism in Hydrophilic Interaction Chromatography

*Sergey M. Melnikov, Alexandra Höltzel, Andreas Seidel-Morgenstern, and Ulrich Tallarek**

Hydrophilic interaction chromatography (HILIC) is the second most important liquid chromatography mode after reversed-phase chromatography, but its retention mechanism has remained largely unknown.[1] HILIC separates polar, hydrophilic analytes between a polar stationary phase, for example bare silica, and an aqueous–organic mobile phase, for which acetonitrile (ACN) has become the solvent of choice. HILIC closes the application gap for compounds that are insufficiently retained on reversed phases, are insoluble in the nonaqueous mobile phases used in normal phase chromatography, and lack the necessary charges for ion-exchange chromatography. Typically for HILIC, retention of analytes requires a predominantly organic mobile phase, and retention often increases steeply at high ACN fractions. Weak adsorptive and possibly electrostatic interactions between analytes and stationary phase contribute to HILIC retention, but its characteristic underlying principle is thought to be the differential partitioning of the hydrophilic analytes between the predominantly organic mobile phase and a quasi-immobilized water layer on the stationary phase (partitioning mechanism).[1,2] The surface adsorption of water onto bare silica stationary phases under HILIC conditions has been studied by chromatographic and spectroscopic methods;[3] however, molecular-level insight into structure and dynamics of the surface water layer is still lacking.

Key contributions to the understanding of reversed-phase chromatography came from molecular dynamics (MD) and Monte Carlo simulations, through the detailed image of the chromatographic interphase region between stationary and mobile phase, where retention of analytes takes place.[4] We now apply this approach to the HILIC system and investigate by MD simulations the composition, structure, and mobility of water/ACN (W/ACN) mixtures inside a 9 nm bare silica pore fed from two adjacent solvent reservoirs (Figure 1). Our model mimics the conditions in a chromatographic column, where more than 99% of the silica surface is inside the mesopores (typical diameters 6–12 nm) of the fixed bed. The W/ACN ratio is varied from 50:50 to 1:99 (v/v) to probe how an increasing ACN fraction in the mobile phase changes the conditions inside the pore.

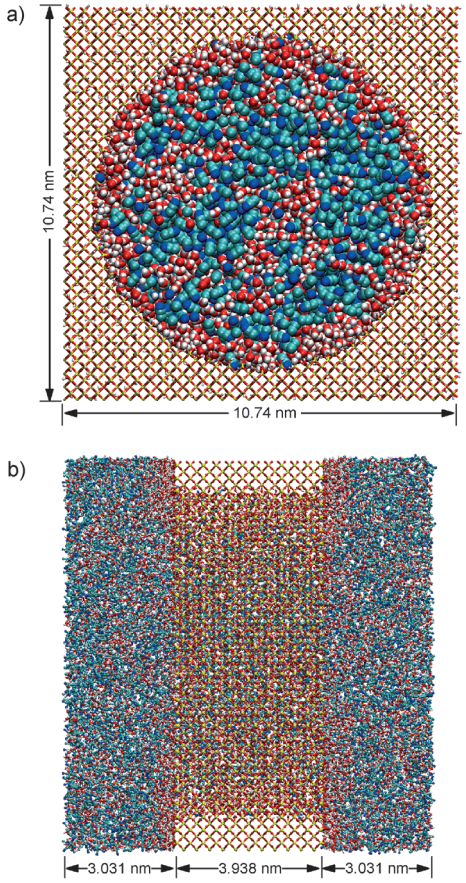

Figure 1. a) Front view (projection) onto the silica block with solvent-filled cylindrical pore of 9 nm diameter. b) Side view (projection) of the simulation box: the pierced silica block is flanked by two solvent reservoirs. The system state is shown after 30 ns simulation time for 30:70 (v/v) W/ACN in the reservoirs. Si: yellow, O: red, H: white, N: blue; central carbon and methyl group of ACN: cyan.

According to the radial number density profiles of the water oxygen atoms, three regions are distinguished in the pore (Figure 2): the immediate surface region (I, $R <$ 0.425 nm), which contains almost exclusively water and only few ACN molecules, the adjacent interface region (II, $R =$ 0.425–1.5 nm), which has high water density towards region I before it relaxes gradually into the pore bulk region (III, $R >$ 1.5 nm), whose radial constant number density profiles match those of the reservoirs.

Region I is governed by the silica surface, whose preference for water molecules relies in the possibility to form a hydrogen bond network that extends from the silanol

[*] Dr. A. Höltzel, Prof. Dr. U. Tallarek
Fachbereich Chemie der Philipps-Universität Marburg
Hans-Meerwein-Strasse, 35032 Marburg (Germany)
E-mail: tallarek@staff.uni-marburg.de
Homepage: http://www.uni-marburg.de/fb15/ag-tallarek
Dr. S. M. Melnikov, Prof. Dr. A. Seidel-Morgenstern
Max-Planck-Institut für Dynamik komplexer technischer Systeme
Sandtorstrasse 1, 39106 Magdeburg (Germany)

Supporting information for this article is available on the WWW under http://dx.doi.org/10.1002/anie.201201096.

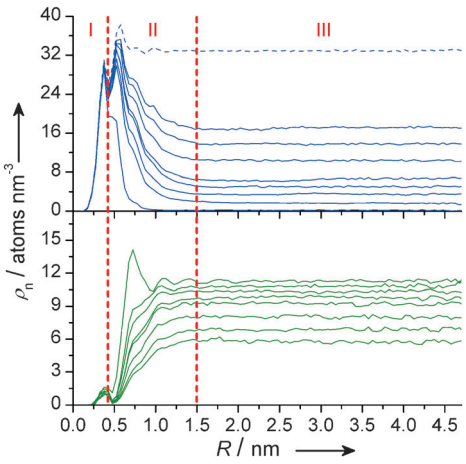

Figure 2. Radial number density profiles for water (oxygen atom; blue) and ACN molecules (central carbon atom; green) inside the silica pore for 100:0 (dashed), 50:50, 40:60, 30:70, 20:80, 15:85, 10:90, 5:95, and 1:99 (v/v) W/ACN in the reservoirs. Dashed red lines indicate the limits of immediate surface region (I), interface region (II), and pore bulk region (III).

groups (SiOH) of the surface towards the pore volume. Nearly all water molecules in region I are directly bound to the surface through W–SiOH hydrogen bonds (HBs) (Figure 3a). In the interface region, the number of W–SiOH HBs then quickly decreases in favor of W–W HBs (Figure 3b). Remarkably, the water coordination peaks at $R \approx 0.7$ nm, just where W–SiOH HBs have ceased; even at low nominal water fraction (5:95 (v/v) W/ACN), the number of W–W HBs per water molecule at this location reaches 80% of the value for pure water. Towards region III, W–W and W–ACN HBs approach values representative of the W/ACN composition in the reservoirs. Figure 3 proves a selective influence of the silica surface beyond the immediate hydrogen bonding range.

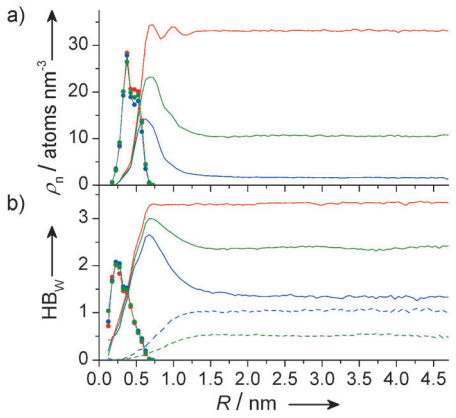

Figure 3. Radial projection of the hydrogen bonding network in the silica pore for 100:0 (red), 30:70 (green), and 5:95 (blue) (v/v) W/ACN in the reservoirs. a) Oxygen atom number density of water molecules directly bound to the surface (by W–SiOH hydrogen bonds; thin lines with dots) and of water molecules not directly connected to the surface (thick lines). b) Average number of hydrogen bonds per water molecule, HB_W, for W–SiOH (thin lines with dots), W–W (thick lines), and W–ACN (dashed) hydrogen bonds.

In the next layer, the presence of W–SiOH HBs favors the formation of W–W rather than W–ACN HBs, which leads to the accumulation of water molecules in the interface region. The microheterogeneity of W/ACN mixtures,[5] that is, the tendency of water and ACN molecules for coordination by their own kind (visible in the pore and the reservoirs of Figure 1), supports this development and explains the success of ACN as organic solvent in HILIC. Figure 3 also shows that coordination of the surface by water molecules takes precedence over formation of the water layer in the interface region: an increasing ACN fraction in the reservoirs hardly matters to the surface-bound water molecules, but decreases the water number density of the non-surface-bound water molecules in the interface region ($R \approx 0.7$ nm) and, though to a lesser degree, their coordination.

With increasing ACN fraction in the reservoirs, the enrichment of water in regions I and II causes the local composition at and near the surface to deviate more and more from the nominal W/ACN ratio (Figure 4). To observe a distinct difference in water content between the region

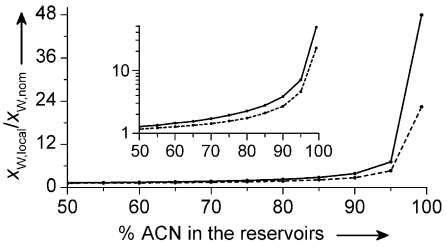

Figure 4. Ratio of local water mole fraction inside the silica pore $x_{W,local}$ (region I: solid, regions I + II: dashed) to the nominal water mole fraction in the reservoirs $x_{W,nom}$ as a function of ACN volume fraction in the reservoirs. Inset: logarithmic plot.

near the silica surface and the reservoirs, however, requires a fairly large nominal ACN fraction, just as retention of polar analytes in HILIC. The local water mole fraction in region I is twice the nominal value at 75% ACN in the reservoirs, and in regions I + II at 85% ACN. Between 95 and 99% ACN, the ratio between local and nominal water mole fraction rises steeply: the striking discrepancy in water fraction between regions I + II and the rest of the system explains why hydrophilic analytes are so strongly retained at high ACN fraction in the mobile phase. Figure 4 is immediately reminiscent of the typical HILIC retention dynamics, which features a shallow increase of analyte retention time over most of the ACN range before the curve ends in an upward sweep at high ACN fraction.[6]

The growing coordination towards the surface through W–W and W–SiOH HBs (Figure 3) affects radial and axial translational mobility of the solvent molecules (Figure 5). The residence time of a solvent molecule at a certain radial distance from the surface increases from $R < 1$ nm towards rather high values in region I. The scarcer the water supply in the reservoirs, the stronger water molecules cling to the surface. For pure water in the reservoirs, water molecules reside ca. 100 times longer in region I than III, and this factor increases to 200, 400, and 600 for 30:70, 5:95, and 1:99 (v/v)

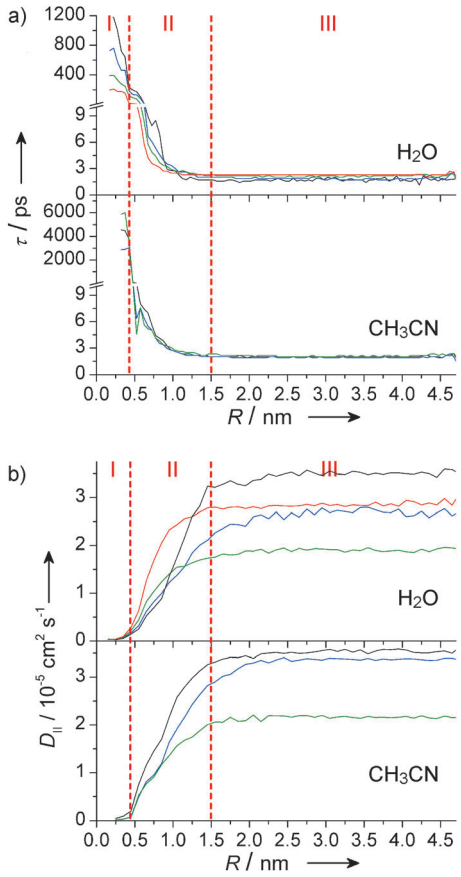

Figure 5. Radial dependence of translational mobility of water and ACN molecules inside the silica pore for 100:0 (red), 30:70 (green), 5:95 (blue) and 1:99 (black) (v/v) W/ACN in the reservoirs. a) Residence time τ at a certain radial distance from the silica surface. b) Diffusion coefficient parallel to the surface ($D_{||}$). Dashed red lines indicate the limits of immediate surface region (I), interface region (II), and pore bulk region (III).

W/ACN, respectively. The few ACN molecules in region I remain even longer, because reaching the pore bulk would involve travel through the high water density layer of the interface region. An attenuated axial mobility of the solvent molecules is observed over a significant distance from the surface: starting as far as the border between pore bulk and interface region ($R \leq 1.5$–2 nm), the diffusion coefficients of water and ACN molecules parallel to the surface and the pore axis decrease towards practically zero in region I.

Owing to the scarce translational mobility of the solvent molecules (Figure 5), the negligible ACN presence, and the independence from the nominal W/ACN ratio in the reservoirs (Figure 2), region I can be interpreted as a quasi-immobilized water layer governed by the silica surface. The interface region (II), whose properties are influenced by the surface as well as by the nominal W/ACN ratio in the reservoirs, is a water-rich layer of reduced translational mobility. Because this description of the situation recalls the electric double layer, region I and II may be designated rigid and diffuse water layer, respectively. The diffuse water layer stretches the pore space region for retention of polar analytes; the retentive layer (regions I + II) accounts for 56% of the 9 nm pore's volume. The reduced mobility in regions I + II is expected to detain analytes in the retentive layer, so that HILIC retention may result from the synergistic effects of solvent composition, structure, and mobility at and near the silica surface.

The present MD study provides a molecular detail basis for HILIC retention of polar analytes through partitioning between an ACN-rich mobile phase and a water layer at the stationary phase:

1. A hydrogen bond network extending from the silanol groups of the silica surface causes accumulation of water molecules and reduction of translational mobility within a distance of ca. 1.5 nm from the surface.
2. The ratio between the local water mole fraction at and near the surface and the nominal water mole fraction grows nonlinearly with the ACN fraction in the mobile phase and ends in a dramatic jump. This behavior matches with the observed HILIC retention dynamics of many polar analytes.
3. The water layer on the stationary phase consists of a rigid and a diffuse part, and as such is at once more complex and more extended than assumed up to now. The formation of the water layer and its structural and dynamic properties can be attributed fundamentally to the hydrogen-bonding capabilities of water, ACN, and the silica surface.

Experimental Section

The simulation box (with dimensions as shown in Figure 1) contained a central block of β-cristobalite SiO_2 with a cylindrical pore of 9 nm diameter. The silica surfaces were prepared as described previously;[7] the surface density of the hydroxyl groups (8.0–8.5 μmol m^{-2}) agrees with typical bare silica stationary phases.[8] MD simulations were performed at 300 K for a canonical NVT ensemble with Gromacs 4.5.2.[9] The force field parameters of Gulmen and Thompson were used for the silica atoms; water was treated with the SPC/E model and ACN with the TraPPE-UA force field.[10] Data analysis was performed on the last 6 ns of a 30 ns long productive simulation run. Further details are compiled in the Supporting Information.

Received: February 9, 2012
Revised: March 9, 2012
Published online: May 8, 2012

Keywords: analytical methods · liquid chromatography · molecular dynamics · partitioning mechanism · retention

[1] a) A. Alpert, *J. Chromatogr. A* **1990**, *499*, 177–196; b) P. Hemström, K. Irgum, *J. Sep. Sci.* **2006**, *29*, 1784–1821; c) M. Lämmerhofer, *J. Sep. Sci.* **2010**, *33*, 679–680; d) Y. Guo, S. Gaiki, *J. Chromatogr. A* **2011**, *1218*, 5920–5938.

[2] a) W. Bicker, J. Wu, H. Yeman, K. Albert, W. Lindner, *J. Chromatogr. A* **2011**, *1218*, 882–895; b) N. P. Dinh, T. Jonsson, K. Irgum, *J. Chromatogr. A* **2011**, *1218*, 5880–5891.

[3] a) D. V. McCalley, U. D. Neue, *J. Chromatogr. A* **2008**, *1192*, 225–229; b) F. Gritti, A. dos Santos Pereira, P. Sandra, G. Guiochon, *J. Chromatogr. A* **2009**, *1216*, 8496–8504; c) J. L. Gasser-Ramirez, J. M. Harris, *Anal. Chem.* **2009**, *81*, 2869–2876; d) E. Wikberg, T. Sparrman, C. Viklund, T. Jonsson, K. Irgum, *J. Chromatogr. A* **2011**, *1218*, 6630–6638.

[4] a) J. L. Rafferty, J. I. Siepmann, M. R. Schure, *Adv. Chromatogr.* **2010**, *48*, 1 – 55; b) S. M. Melnikov, A. Höltzel, A. Seidel-Morgenstern, U. Tallarek, *J. Phys. Chem. C* **2009**, *113*, 9230 – 9238.
[5] R. D. Mountain, *J. Phys. Chem. B* **2010**, *114*, 16460 – 16464.
[6] The exact curve progression depends on the analyte and the actual experimental conditions. See, for example: a) Figure 2 in E. S. Grumbach, D. M. Diehl, U. D. Neue, *J. Sep. Sci.* **2008**, *31*, 1511 – 1518; b) Figure 2 in F. Gritti, A. dos Santos Pereira, P. Sandra, G. Guiochon, *J. Chromatogr. A* **2010**, *1217*, 683 – 688; c) Figure 1 in A. E. Karatapanis, Y. C. Fiamegos, C. D. Stalikas, *J. Chromatogr. A* **2011**, *1218*, 2871 – 2879.
[7] S. M. Melnikov, A. Höltzel, A. Seidel-Morgenstern, U. Tallarek, *Anal. Chem.* **2011**, *83*, 2569 – 2575.
[8] U. D. Neue, *HPLC Columns*: *Theory*, *Technology*, *and Practice*, Wiley-VCH, Weinheim, **1997**, p. 110.
[9] D. van der Spoel, E. Lindahl, B. Hess, G. Groenhof, A. E. Mark, H. J. C. Berendsen, *J. Comput. Chem.* **2005**, *26*, 1701 – 1718.
[10] a) T. S. Gulmen, W. H. Thompson, *Langmuir* **2006**, *22*, 10919 – 10923; b) H. J. C. Berendsen, J. R. Grigera, T. P. Straatsma, *J. Phys. Chem.* **1987**, *91*, 6269 – 6271; c) C. D. Wick, J. M. Stubbs, N. Rai, J. I. Siepmann, *J. Phys. Chem. B* **2005**, *109*, 18974 – 18982.

